archaeometry

Archaeometry ••, •• (2017) ••–•• doi: 10.1111/arcm.12291

MAGNETIC ALTERATION OF SOILS BY LATE HOLOCENE HUNTER–GATHERER GROUPS (TIERRA DEL FUEGO, SOUTH AMERICA)*

I. L. OZÁN,† M. J. ORGEIRA, C. VÁSQUEZ and M. NASELLI

Instituto de Geociencias Básicas, Aplicadas y Ambientales de Buenos Aires, Consejo Nacional de Investigaciones Científicas y Tecnológicas, Departamento de Ciencias Geológicas, Universidad de Buenos Aires, Pabellón 2, Ciudad Universitaria (C1428EGA), Buenos Aires, Argentina

The present work aims to analyse the magnetic signature from the Late Holocene open-air archaeological deposits of hunter–gatherer ephemeral occupations. For this purpose, two profiles were sampled at the Marazzi 2 site in the north-western Isla Grande de Tierra del Fuego, Chile, in order to carry out studies of magnetic susceptibility, hysteresis cycles, back-field remanent magnetization, isothermal remanent magnetization and thermal variation of magnetic susceptibility at high and low temperature. Despite short-term occupations, the P1 profile shows a magnetic peak at a depth of ~30–70 cm due to magnetite, probably formed by anthropogenic activity related to combustion. The P2 profile instead yields an anomalous peak of coercivity (at a depth of 20–40 cm), which could also be anthropogenic, due to the presence of finely dispersed ancient 'red ochre'. The red ochre is proposed to form anthropogenic thermal alteration of goethite associated with volcanic ash, the remnants of which were found in thin sections from the P2 subsoil.

KEYWORDS: HUNTER–GATHERERS, OPEN-AIR SITE, MAGNETIC ENHANCEMENT, COMBUSTION, OCHRE

INTRODUCTION: SOIL MAGNETISM AND ARCHAEOLOGICAL SITES

The Marazzi 2 site (MA2) is a costal open-air archaeological settlement, which occupies an area of ~800 000 m^2 (Fig. 1). Its archaeological record indicates several ephemeral but periodic occupations of hunter–gatherer groups since *c.* 3000 BP until the European arrival (Ozán *et al.* 2015). Most of the archaeological record is buried in polycyclical soil profiles up to ~160 cm deep, a rare characteristic in the regional context. This work aims to analyse the magnetic signal of two soil profiles of MA2, in order to discuss the impact of low demography and highly mobile populations on soil magnetic properties.

The natural magnetic signal in soils is a consequence of external factors, such as climate, and internal organic and inorganic interactions occurring in soil horizons. According to the magnetic response, materials are classified into diamagnetic, paramagnetic, ferromagnetic, antiferromagnetic and ferrimagnetic (Maher and Thompson 1999; Peters and Dekkers 2003). Changes in magnetic properties can result from changes in the type and abundance of magnetic mineralogy, as well as its particle size. A small proportion of ferromagnetic minerals (e.g., magnetite, titanomagnetite) is enough to dominate the soil magnetic signature.

Ultra-fine magnetite formation in soils is a well-documented phenomenon. The process requires the oxidation of Fe^{2+} dissolved in a pH value of around 7 (Taylor *et al.* 1987; Maher

*Received 20 June 2016; accepted 18 October 2016
†Corresponding author: email ivanalozan@gmail.com

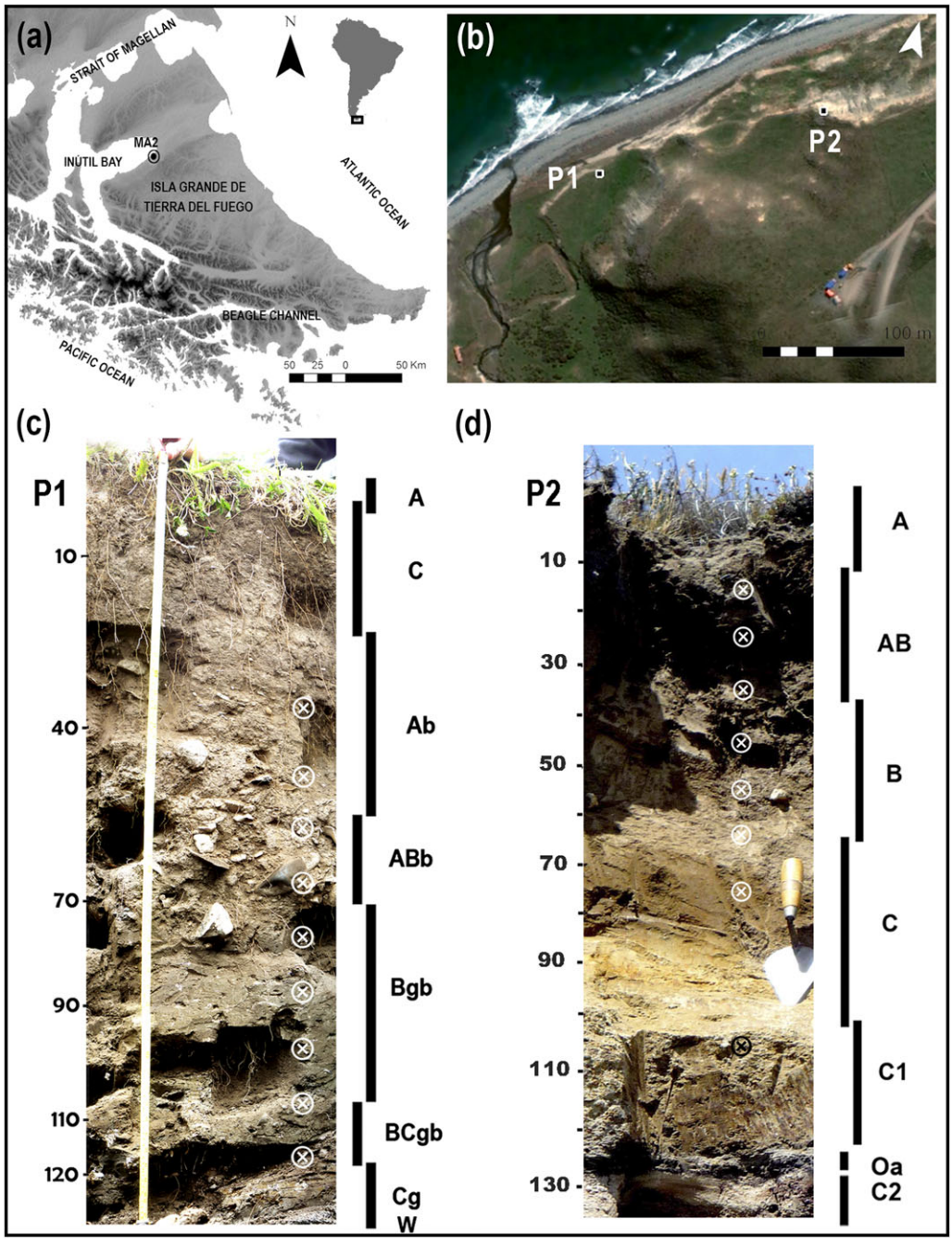

Figure 1 *Isla Grande de Tierra del Fuego: (a) the Marazzi 2 site (S53°31.508′ W69°21.661′); (b) a satellite image showing the two studied profiles; (c) profile 1 (P1); (d) profile 2 (P2). Sample positions (crosses) are shown on (c) and (d); scale in cm. [Colour figure can be viewed at wileyonlinelibrary.com]*

1988). Fe^{2+} ions are liberated during Fe silicate weathering due to wet/dry cycles, and the presence of oxygen transforms Fe^{2+} into Fe^{3+}. By hydrolysis and subsequent polymerization, Fe^{3+} precipitates as poorly crystallized oxyhydroxides such as ferrihydrite ($Fe_5HO_8{\cdot}4H_2O$), which in turn are reduced by soil bacterial action under anaerobic conditions (e.g., Lovley *et al.* 1987; Fischer 1988; Maher 1998; Dearing *et al.* 2001; Maher *et al.* 2003; Banerjee 2006). The formation of magnetite and other iron minerals is the final result of this process and, in effect, the main reason for soil magnetic enrichment (Tamaura *et al.* 1983, Tronc *et al.* 1992). Earlier, much effort has been invested to understand the diversity and significance of palaeosol magnetic enhancement in loess/palaeosol sequences in China (Kukla *et al.* 1988) and elsewhere (Evans and Heller 2003) for global Quaternary correlations. More recent endeavours allowed Orgeira *et al.* (2011) to propose a robust model to calculate palaeo-precipitation from the data on pedogenic magnetic susceptibility. This model of magnetic enhancement in soils also applies to subaerial anthropogenic deposits in the studied archaeological sites.

The formation and destruction of pedogenetic magnetite is conditioned by multiple soil internal factors such as drainage, texture, average pH, redox conditions, organic matter abundance, soil microclimate, cation exchange capacity and parent material composition (Orgeira *et al.* 2011). The magnetic signal is also related to climatic variables such as precipitation and temperature (e.g., Heller *et al.* 1993; Maher *et al.* 1994; Liu *et al.* 1995). However, the magnetic behaviour does not have a linear correlation with climatic variability, and 'thresholds' have been proposed in order to explain the magnetic–climate interaction (Han *et al.* 1996; Orgeira and Compagnucci 2006, 2010; Orgeira *et al.* 2011).

As humans modify soils, they are also an important cause of soil magnetic signature modification. Urban activities, industry and modern agriculture have a substantial impact on soil magnetic properties (e.g., Chaparro 2006). However, pre−/non-industrial populations also modified soil properties by the intentional or unintentional incorporation of organic matter, activities giving rise to combustion and/or the manufacture of specific technologies associated with iron oxides, such as metallurgy and pigment preparation. Since the pioneering contribution of Le Borgne (1960), several authors have demonstrated that natural or anthropogenic fires in soils produce anaerobic conditions capable of promoting magnetite precipitation (or maghemite after oxidation) under certain organic matter thresholds and in the presence of iron (e.g., Aitken 1970; Tite and Mullins 1971; Mullins 1974; Fitzpatrick 1985; Maher 1986; Maher and Taylor 1988). Dalan and Banerjee (1998) and Dalan (2008) exhaustively revised the broad applicability of magnetic properties in archaeological contexts, which can be summarized as follows:

(1) Magnetic properties as the definition of activity areas, functionality, building strategies, pigment sources and intensity of human occupation (e.g., Oldfield *et al.* 1985; Allen and Macphail 1987; Clark 1990; Dockrill and Simpson 1994; Gose *et al.* 1994; Crowther and Barker 1995; Dalan 1997; Marmet *et al.* 1999; Orgeira *et al.* 2000; Crowther 2003; Mooney *et al.* 2003; Goldberg and Macphail 2006; Macphail and Crowther 2007; Rosendahl *et al.* 2014; Ozán and Orgeira 2015; Tsatskin and Gendler 2016).
(2) Magnetic properties as chronological frames. In archaeological stratigraphies, palaeomagnetism can be used as a chronological indicator due to the presence of a known aged magnetic feature (e.g., Evans 1977; Tarling 1983; Schmidbauer *et al.* 1986; Moskowitz *et al.* 1987; Eighmy and Sternberg 1990; Nami 1995; Chiari and Lanza 1997; Borradaile *et al.* 1998; Ellwood *et al.* 2004).
(3) Magnetic proxies for pedogenetic, geomorphological dynamic, natural fire occurrence and post-depositional processes. As upper soil horizons and surfaces affected by fire may have a distinctive magnetic signal, magnetic studies are palaeoenvironmental proxies. In

archaeological contexts, these data are useful to understand natural scenarios where the human action took place (e.g., Thompson and Oldfield 1986; Almgren 1989; Brown 1992; Ollendorf 1993; Lageras and Sandgren 1994; Orgeira *et al.* 2000; Tsatskin and Nadel 2003; Goguitchaichvili *et al.* 2011).

The study area

The Marazzi 2 site is located along the south-eastern coast of the Inútil Bay of the north-western steppe of Tierra del Fuego, Chile (Fig. 1 (a)). The area has a mean annual temperature of ~6°C. Rainfall is around 300 mm per year and westerly winds, which are more intense in the summer, reach an average of ~60 km/h. These conditions result in a semi-arid cold steppe environment with a maritime influence.

Mainly as a consequence of these climatic conditions, soil profiles are very weakly developed, with an A–AC–C soil profile often beneath aeolian and colluvial sediments, on which there is incipient pedogenesis exhibiting an A–C profile. Sedimentological and edaphic descriptions have been reported previously (Ozán *et al.* 2015).

Profile P1 is situated on a fluvial terrace of the Torcido river, near a river valley slope and beyond a terminal moraine (Fig. 1 (b)). This profile is part of an excavation unit that has been subject to previous excavations since 2002, which rendered information concerning ~1.5 m of continuous archaeological deposits (stone artefacts, bones, mollusc shells, charcoal, ash and red ochre) and constitutes one of the deepest human-related sedimentary records in northern and central Tierra del Fuego (Morello *et al.* 1998, 2004). Profile P2 is in a 2.70 m front cliff, although only the upper 1.3 m were analysed for this work (Fig. 1 (b)). Archaeological material only appears between 10 and 65 cm deep (Morello *et al.* 1998), whereas a volcanic ash layer at about 75 cm deep is microscopically recorded (Ozán and Orgeira 2015).

METHODOLOGY

In P1 and P2, nine and eight sedimentological samples, respectively, were taken at 10 cm intervals along the profiles (see positions in Fig. 1 (c) and (d)). The sedimentological and edaphological descriptions have been the subject of previous contributions (Ozán *et al.* 2015).

Magnetic susceptibility was measured using an AGICO (Advance Geoscience Instrument Company, Czech Republic) susceptibility meter, model MFK1-FA, at a frequency of ~1000 Hz (at 200 A m^{-1}, the maximum amplitude of the magnetic field). For some samples, the magnetic susceptibility was measured at different frequencies (1000 and 4000 Hz) and fields (from low fields up to 700 A m^{-1}) in order to identify magnetic minerals and to infer the grain-size distribution (Liu *et al.* 2005; Hrouda 2009, 2011).

Before measuring, dried samples were ground in an agate mortar. The susceptibility values were normalized to mass. Hysteresis loops and magnetization with reverse field were run in the vibrating sample magnetometer (VSM, Molspin Ltd). The data allowed the calculation of the saturation remanent magnetization (M_{rs}), the saturated magnetization (M_s), the coercivity of remanence (H_{cr}) and the coercivity (H_c). The isothermal remanent magnetization (IRM) was run using an AGICO instrument, model JR-6 dual speed spinner magnetometer, and an ASC Scientific impulse magnetizer, model IM-10-30. For these measurements, samples were consolidated with epoxy resin.

The extensive parameters (X, M_s and M_{rs}) enable estimation of the type, amount and size of magnetic minerals. For example, high-coercivity minerals are antiferromagnetic (e.g., hematite

and goethite), while low coercivity is characteristic of ferrimagnetic minerals (e.g., magnetite and titanomagnetite). The calculation of rock-magnetic parameters such as X/M_s, H_{cr}/H_c and M_{rs}/M_s helps to identify variations in the particle size of the magnetic minerals.

In order to study the various forms of magnetic behaviour, the thermal variation of the magnetic susceptibility was evaluated for a set of selected samples (2–2, 2–3 and 2–7), at high and low temperature in an argon atmosphere. For this purpose, an AGICO model MFK1-A Multifunction Kappabridge was used.

RESULTS

Table 1 presents the magnetic parameters, the pH values and an estimation of the archaeological record abundance corresponded to P1 and P2 archaeological profiles. With a few exceptions, the main magnetic minerals are magnetite and/or titanomagnetite, according to the H_c and H_{cr} values. The hysteresis loops (Fig. 2 (a, b and c)) and the *S*-ratio (IRM-300 mT/IRM-1000 mT) indicate a dominance of low-coercivity minerals (ferrimagnetic) and a subordinated fraction of high-coercivity ones. Some wasp-waisted hysteresis loops suggest a predominance of low-coercivity minerals (Roberts *et al.* 1995).

The extensive magnetic parameters are higher in the upper part of the P1 profile (between 30 and 70 cm) due to the magnetic mineral concentration and/or the magnetic particle size suggested by the X/M_s ratio between depths of 30 and 50 cm. Minor oscillations of the extensive parameters (X, M_s and M_{rs}) are registered in the P2 profile, with the exception of two peaks at depths of about 20–30 cm and 70–80 cm (samples 2–3 and 2–7). The first (2–3) coincides with an outstanding increase of H_{cr}, the origin of which should be attributed to the presence of high-coercivity minerals. The second increase (2–7) could be related to the presence of a volcanic glass, which was identified in petrographic thin sections (see Fig. 3 (h)) containing magnetite or titanomagnetite.

High H_{cr} values (samples 2–2 and 2–3; Table 1) were first considered anomalies, but repeated measurements strongly confirm the initially obtained high values. Therefore, the presence of high-coercivity magnetic minerals must be considered.

The IRM curves reflect three distinctive behaviours (Fig. 2 (e)). On the one hand, samples with higher M_{rs} values indicate an abundance of ferrimagnetic minerals, which coincides with an intensive human occupation level (samples 1–2, 1–3 and 1–4; Figs. 3 (a) and 3 (c)) and a layer with a volcanic input (sample 2–7; Fig. 3 (h)). On the other hand, the IRM curves with lower M_{rs} values are associated with magnetic signal depletion due to groundwater oscillations (sample 1–9) and a temporal lacustrine body (sample 2–8). Finally, a third cluster of samples show an intermediate behaviour related to the mixture of high- and low-coercivity magnetic minerals.

In cases of Ti-poor ferrimagnetic minerals (titanomagnetite or pure magnetite), the M_{rs}/M_s and H_{cr}/H_c ratios allow the estimation of the magnetic particle size. The P1 profile shows a predominance of pseudo-single-domain (PSD) particles, with one single-domain (SD) sample at the bottom (1–9), and two samples with a mixture of SD plus superparamagnetic (SP) grains (1–3 and 1–4) (Dunlop 2002; see Fig. S1). However, determinations of magnetic susceptibility at different frequencies do not show significant differences between the samples (Table 2), which in fact results from the grain-size mixture, which is apparently more complex than first suggested (Dunlop 2002).

The P2 profile also presents PSD particles with some multi-domain (MD) grains (2–2, 2–3 and 2–5), one SD sample at the bottom (SD) and two SD + SP particles (2–4 and 2–7). Anomalously high H_{cr}/H_c ratios in MD samples (2–2, 2–3 and 2–5; see Fig. S1) could be associated with mixtures of magnetic minerals of different and contrasting coercivities (Jackson 1990); for example, magnetite plus hematite or goethite. Determinations of magnetic susceptibility at different

Table 1 *The magnetic susceptibility, X (at 1000 Hz; m^3/kg); the saturated magnetization, M_s (Am^2/kg); the saturation remanent magnetization, M_{rs} (Am^2/kg); the coercivity, H_c (mT); the remanence coercivity, H_{cr} (mT); and the ratios between them (M_{rs}/M_s, H_{cr}/H_c, X/M_s and $S = S_{ratio}/100$ Hz). The abundance of the archaeological record (AR) was quali-quantitatively estimated according to various publications (Morello et al. 1998; Calás and Lucero 2009; Ozán et al. 2015). L, lithics; B, bone fragments (NISP); M, molluscs (MNI); C, charcoal; A, ash*

Sample (depth, cm)	*Magnetic parameters*									*pH*	*AR*
	X ($\times 10^{-7}$)	M_s ($\times 10^{-2}$)	M_{rs} ($\times 10^{-2}$)	H_c	H_{cr}	M_{rs}/M_s	H_{cr}/H_c	X/M_s ($\times 10^{-5}$)	S_{ratio}		
Profile P1											
1–1 (~35)	13.6	1.9	0.2	11.6	26.5	0.19	2.3	7.16	0.9	7.7	L: 514 B: 1168
1–2 (~45)	16.8	3.0	0.1	4.7	22.9	0.03	4.9	5.60	0.9	8	M: 1814 C: xxx
1–3 (~55)	18.2	6.1	0.5	2.9	16.3	0.08	5.7	2.98	0.4	8.2	A: x O: x
1–4 (~65)	14.7	5.0	0.4	2.1	29.4	0.08	13.7	2.94	1	8.3	L: 197 B: 692
1–5 (~75)	6.8	2.0	0.1	7.8	26.8	0.05	3.4	3.40	1	8.2	M: 2724 C: x
1–6 (~85)	6.4	2.3	0.2	8.4	26.8	0.07	3.1	2.78	1	8	A: xxx O: x
1–7 (~95)	5.8	1.8	0.1	7.0	27.0	0.07	3.8	3.22	0.9	8.2	L: 61 B: 105
1–9 (~150)	1	0.5	0.3	13.0	27.7	0.60	2.1	2.00	0.9	6.7	M: 704 C: xx A: – O: x

Sample (depth, cm)	*Magnetic parameters*									*pH*	*AR*
	X ($\times 10^{-7}$)	M_s ($\times 10^{-2}$)	M_{rs} ($\times 10^{-3}$)	H_c	H_{cr}	M_{rs}/M_s	H_{cr}/H_c	X/M_s ($\times 10^{-5}$)	S_{ratio}		
Profile P2											
2–1 (~12)	11.74	2.5	0.5	5.9	24.3	0.02	4.1	4.70	0.9	6.8	L: xx B: 132
2–2 (~25)	11.23	8.2	0.3	2.6	332.6	0.004	128.2	1.37	0.9	7	M: 9 C: xxx
2–3 (~35)	17.93	7.0	0.5	2.0	147.8	0.01	72.6	2.56	0.9	6.8	A: – O: xxx
2–4 (~45)	9.57	6.5	0.8	2.2	23.7	0.01	10.8	1.47	1	6.9	L: x
2–5 (~55)	10.7	5.1	0.5	1.3	39.9	0.01	30.6	2.10	0.9	6.9	B: 15 M: 2
2–6 (~65)	8.47	2.5	1.1	6.0	26.1	0.04	4.3	3.39	0.9	7.2	C: x A: –
2–7 (~75)	17.7	4.0	5.3	3.7	41.6	0.13	12.7	4.42	0.9	6.7	O: –
2–8 (~110)	7.25	0.7	3.7	24.8	27.3	0.52	1.1	1.00	0.9	4.1	Sterile

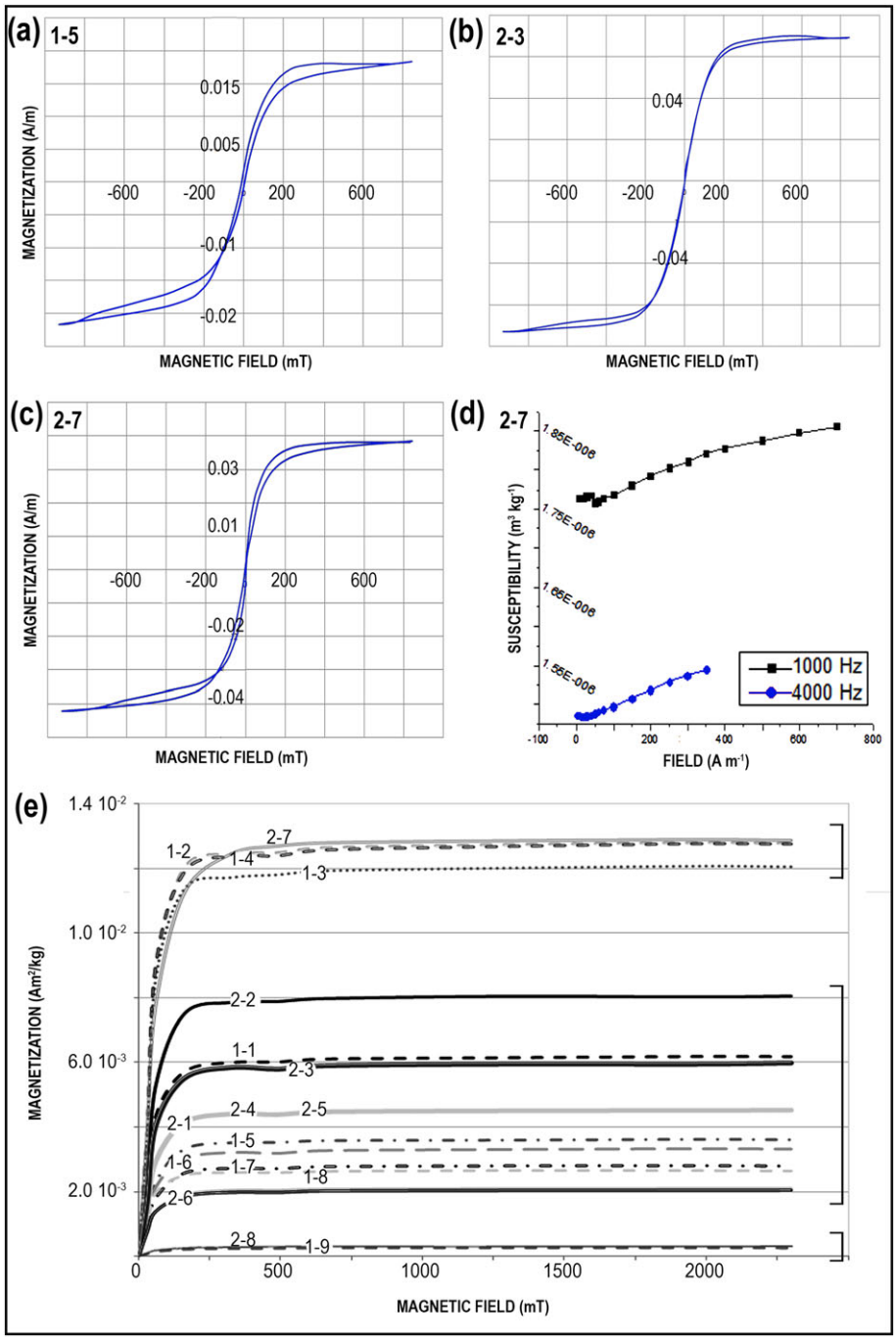

Figure 2 *(a, b, c) Examples of hysteresis loops from the two profiles. (d) An example of a frequency-dependent susceptibility increase in sample 2–7 with respect to a growing magnetic field, note susceptibility increase linearity. (e) IRM curves. [Colour figure can be viewed at wileyonlinelibrary.com]*

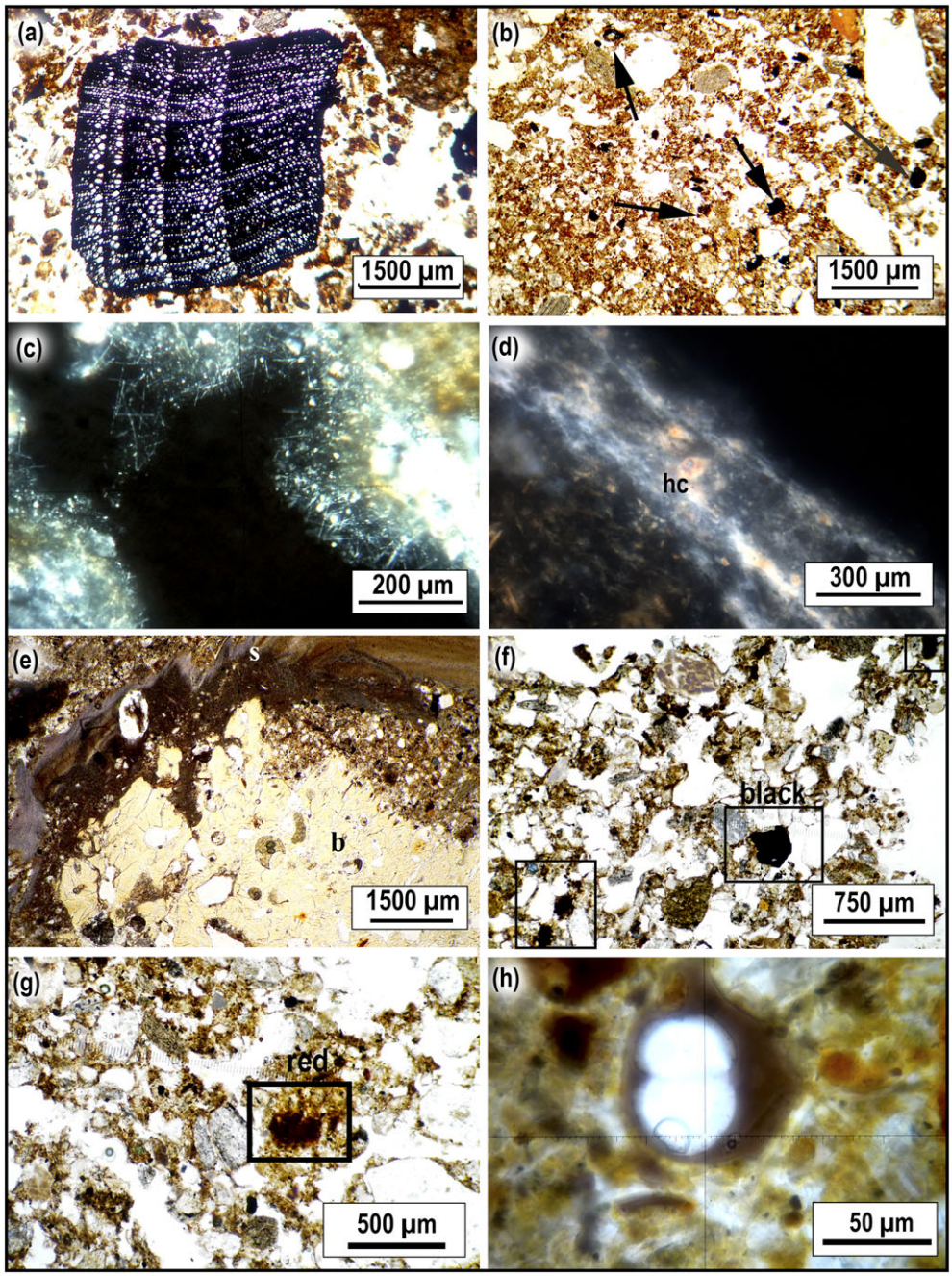

Figure 3 *Microphotographs (PPL, plane-polarized light; XPL, cross-polarized light): (a) anthropogenic charcoal (PPL, P1, 28–41 cm); (b) opaque minerals (arrows) probably containing magnetite (PPL; P1, 44–55 cm); (c) calcitic ash produced by anthropogenic combustion (XPL; P1, 63–75 cm); (d) hypocoating of depletion of Fe and Mn (XPL; P1, 86–99 cm); (e) the dissolution process of bone "b" and shell "s" (PPL; P1, 112–124 cm); (f) opaque minerals (squares) interpreted as magnetite (PPL; P2, 18–30 cm); (g) iron oxide impregnation (Fe^{3+}, square), also presented in other spots of the slide (PPL; P2, 30–43 cm); (h) volcanic glass (PPL; P2, 62–82 cm). [Colour figure can be viewed at wileyonlinelibrary.com]*

Table 2 *The mass susceptibility, χ, and the frequency-dependent susceptibility, χ_{fd}, in selected samples: n/s, not significant*

Sample	*Mass susceptibility, χ (m^3/kg^{-1}, $\times 10^{-6}$)*	*χ_{fd} (%)*
1–3	2.12	n/s
1–4	1.39	n/s
2–4	0.95	n/s
2–5	0.99	29.6 ± 0.3
2–7	1.79	15.5 ± 0.3

frequencies show substantive differences between measurements, which definitely confirms the presence of SP particles (Table 2). In sample 2–7, the susceptibility difference $\chi_{fd} = (15.5 \pm 0.3)\%$ is in agreement with the presence of ultra-fine grains of maghemite with grain sizes in the SP range (diameters <30 nm; Muxworthy and Williams 2006), which could be a by-product of diagenetic and/or weathering processes. As an example, Figure 2 (d) also presents the behaviour of sample 2–7: the increase in the susceptibility with a growing magnetic field is linear and may be attributed to detrital titanomagnetite with a medium titanium content. Sample 2–5 shows unusually high χ_{fd} values near 30%, which is normally taken as an indication of SP grains. It has to be considered here that the mass susceptibility is roughly the same in all the samples, ranging between 2.12×10^{-6} and $0.95 \times 10^{-6}\,m^3\,kg^{-1}$; therefore, the variation in the mass magnetic susceptibility presented in Table 2 is probably not a function of SP grains only.

Figure 4 exhibits low- and high-temperature thermomagnetic curves for four samples of the P2 profile in order to better understand their magnetic behaviour, especially taking the high H_{cr} values into account. The curve for synthetic goethite is also presented in Figure 4 as a reference. The high-temperature thermomagnetic curve of sample 2–2 is compatible with magnetite, whereas its low-temperature curve shows a Verwey transition, which corresponds to the presence of MD magnetite. Samples 2–3 and 2–7 show a behaviour similar to that of synthetic goethite, while the low-temperature curve of sample 2–3 presents a noisy behaviour. Sample 2–7 shows a peak near 250°C in the heating and cooling curve, which could be attributed to the presence of TM40 (titanomagnetite with 40% of titanium; Moskowitz *et al.* 1998), whereas a broad peak at 525°C near the Curie point of magnetite could be due to chemical reduction of maghemite to magnetite during the laboratory treatment. Thus, according to this technique, this sample has a mixture of magnetite plus goethite. Its cooling curve indicates a Hopkinson peak at 520°C (Gajbhiye *et al*. 1999), probably due to the neo-formation of ultra-fine single-domain grains of magnetite from iron-containing minerals during the laboratory heating processes.

The thermomagnetic curve of sample 2–5, like the one for sample 2–7, shows a broad Verwey peak that can be attributed to maghemitized MD magnetite (Fig. 4). Also, it could be indicative of weathering processes on detrital grains, while the Hopkinson peak can be due to neo-formation of magnetic minerals during the laboratory heating processes. Again, sample 2–5 shows an irreversible thermomagnetic curve due to transformations of magnetic minerals during the laboratory heating processes.

DISCUSSION

The relatively high-*X* magnetic susceptibility registered in the P1 profile at a depth of ~30–70 cm coincides with a high abundance in the archaeological record, which provides evidence of combustion, including burnt bones, charcoal and ash (Table 1, Figs 3 (a) and 3 (c)). Therefore, it is

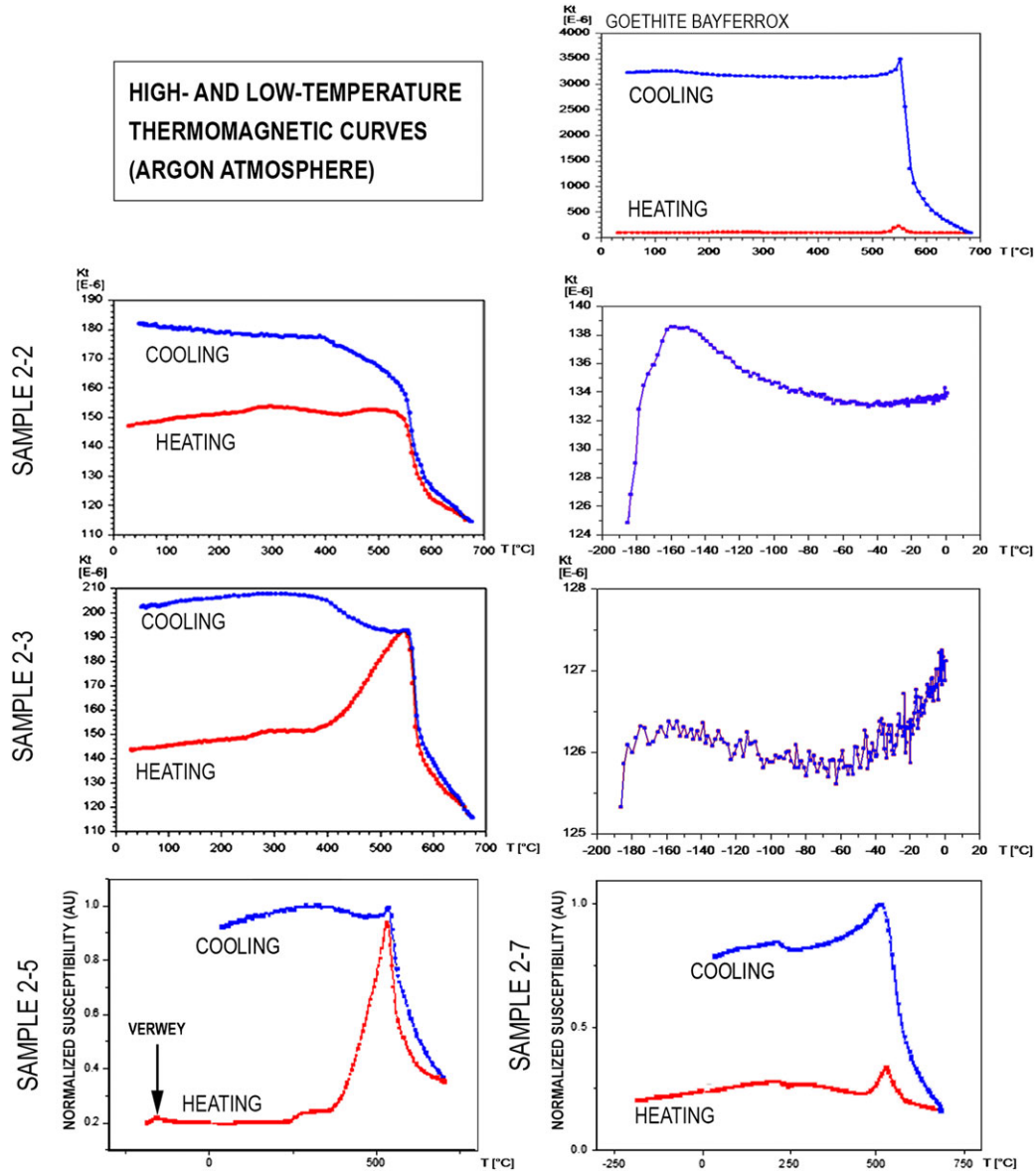

Figure 4 *High- and low-temperature thermomagnetic curves, in argon atmospheres. [Colour figure can be viewed at wileyonlinelibrary.com]*

proposed that this anthropogenic combustion may have caused magnetite enhancement (Fig. 3 (b); Dalan and Banerjee 1998; Marmet *et al.* 1999; Macphail and Crowther 2007). In addition, the presence of SP particles (1–3 and 1–4; Fig. S1) could be related to such anthropogenic activity. Pedogenetic processes would also alter detrital ferrimagnetic minerals under certain conditions not registered here, such as moderate/abundant precipitation, a high organic matter content, relatively acid pH values and/or pore rich-silica water (Orgeira *et al.* 2011). In contrast to these upper layers, the magnetic signal beneath them (between sample 1-5 and 1-9) seems to

be dominated by natural processes. In fact, the presence of hypocoatings of depletion (Fig. 3 (d)) and evidence of dissolution (Fig. 3 (e)) below ~70 cm indicates intensive illuviation (Bbg) and groundwater oscillation, respectively. It has to be emphasized that this Bbg horizon corresponds to a soil profile that developed under environmental conditions (climatic and/or geomorphological) that were different from the present ones (Ozán *et al.* 2015).

According to the results presented above, samples 2–7 and 2–3 show a thermomagnetic behaviour compatible with goethite. Sample 2–7 sample, as well as sample 2–5, shows a Curie temperature of magnetite which, along with the presence of SP particles, suggests the inclusion of magnetite in volcanic glass registered in that level. The goethite contained in sample 2–7 could be attributed to different processes related to weathering.

On the other hand, the high coercivity and coercivity ratio in sample 2–3 are consistent with mixtures of magnetic minerals; for example, in the form of magnetite plus hematite or goethite. In the latter case, the magnetite is MD, so it is detrital; the goethite or hematite could be attributable to various weathering and/or anthropogenic processes.

The results obtained for sample 2–2 suggest that the MD magnetite may have occurred along with a high-coercivity mineral.

The anomalous H_{cr} values of the P2 profile at a depth of about 20–40 cm (samples 2–2 and 2–3) could correspond to a layer with a magnetic mixture, including hematite (very fine particles, 5–25 μm; De Boer 1999). This H_{cr} peak coincides with a slight increment of M_s, a decrease in the *S*-ratio and the maximum abundance in the archaeological record (Table 1). Additionally, thin sections of soil micromorphology show the presence of iron oxide impregnations and opaque minerals (Figs. 3 (f) and 3 (g)). Interestingly, an archaeological excavation undertaken 15 m from the P2 profile (Morello *et al.* 1998) reported the presence of 'red ochre' at a depth of ~15–30 cm. Normally, materials from prehistoric hearths accumulate not only magnetite but also hematite with a strong colouring power, which could have been used as a red pigment.

After the arrival of Europeans in Tierra del Fuego, the ethnohistorical descriptions—which include a broad photograph record—highlight the use of red, black and white pigments as colouring substances for body-painting and other activities (e.g., Fiore 2014 and references therein). Archaeologically, the presence of these pigments is rare, although some studies have found red substances on rocks and sediments (Fiore *et al.* 2008). These authors carried out chemical analysis in order to analyse the organic and inorganic composition of red pigments at archaeological sites from southern Tierra del Fuego. The results showed variations of hematite and lipids as blenders, whereas regional off-site studies did not find the source of the hematite present at the archaeological sites (Fiore *et al.* 2008).

It is thus proposed that the possible anthropogenic hematite present in the P2 profile, and probably at other sites in the region, was not directly obtained from a natural source (on- or off-site), but was synthesized by pyrogenic technologies (Tsatskin and Gendler 2016). In this sense, the provenance studies in search of hematite raw material sources should consider geochemical and magnetic modifications that occur during sediment combustion (Mooney *et al.* 2003). Past populations probably looked for sediments the thermal management of which might produce red colours (hematite or goethite plus hematite), such those containing goethite that formed as a consequence of the abundant volcanic weathered material (sample 2–7; Fig. 3 (h)), a common feature along the Isla Grande de Tierra del Fuego.

CONCLUSIONS

Despite being widely applied at archaeological sites, the applicability of magnetic properties at open-air sites in highly mobile hunter–gatherer contexts comprises a particular challenge due

to the ephemeral character of the human occupations, and intemperization may obscure the magnetic anthropogenic enrichment. However, the aggradational pedogenesis and semi-arid conditions at MA2 offer good preservational conditions for the archaeological record and for human soil signatures.

The present case study also suggests that magnetic methods may help to identify high-coercivity minerals (e.g., goethite and hematite) that are the main constituents of paints. In Tierra del Fuego, hematite may have been obtained via the combustion, either intentional or unintentional, of goethite-rich sediments. In this case, archaeologists are advised to explore the technological processes of hematite production more deeply, along with seeking the geological sources of ochre in the nearby surrounding. However, our results are as yet preliminary and deserve additional research effort in the future.

ACKNOWLEDGMENTS

We are grateful to Sebastián Oriolo for his invaluable help in the general preparation of the manuscript. This work was supported by a Pluriannual Investigation Projects (PIP 0573) grant, from the National Council of Science and Technology, and by a University of Buenos Aires—Science and Technology (UBACyT 20020130100146BA) grant.

REFERENCES

Aitken, M. J., 1970, Magnetic location, in *Science in archaeology* (eds. D. Brothwell and E. Higgs), 681–94, Praeger, New York.

Allen, M. J., and Macphail, R. I., 1987, Micromorphology and magnetic susceptibility studies: their combined role in interpreting archaeological soils and sediments, in *Soil micromorphology* (eds. N. Fedoroff, L. Bresson, and M. Courty), 669–76, Association Française pour l'Étude du Sol, Plaisir.

Almgren, E. B., 1989, Woodland establishment, expansion, and regression in association with prehistoric and later human settlements around Lough Gur, Co. Limerick, Ireland, Ph.D. thesis, University of Minnesota.

Banerjee, S. K., 2006, Environmental magnetism of nanophase iron minerals: testing the biomineralization pathway, *Physics of the Earth and Planetary Interiors*, **154**, 210–21.

Borradaile, G. J., Stewart, J. D., and Ross, W. A., 1998, Characterizing stone tools by rock-magnetic methods, *Geoarchaeology: An International Journal*, **13**, 73–91.

Brown, A. G., 1992, Slope erosion and colluviation at the floodplain edge, in *Past and present soil erosion: archaeological and geophysical perspectives* (eds. M. Bell and J. Boardman), 77–87, Oxbow Monograph 22, Oxbow Books, Oxford.

Chaparro, M., 2006, *Estudio de parámetros magnéticos de distintos ambientes relativamente contaminados en Argentina y Antártida*, Ed, Geofísica UNAM, Buenos Aires.

Chiari, G., and Lanza, R., 1997, Pictorial remanent magnetization as an indicator of secular variation of the Earth's magnetic field, *Physics of the Earth and Planetary Interiors*, **101**(1), 79–83.

Clark, A. J., 1990, *Seeing beneath the soil: prospecting methods in archaeology*, Batsford, London.

Crowther, J., 2003, Potential magnetic susceptibility and fractional conversion studies of archaeological soils and sediments, *Archaeometry*, **45**, 685–701.

Crowther, J., and Barker, P., 1995, Magnetic susceptibility: distinguishing anthropogenic effects from the natural, *Archaeological Prospection*, **2**, 207–15.

Dalan, R. A., 1997, The construction of Mississippian Cahokia, in *Cahokia: domination and ideology in the Mississippian world* (eds. T. Pauketat and T. Emerson), 89–102, University of Nebraska Press, Lincoln, NE.

Dalan, R. A., 2008, A review of the role of magnetic susceptibility in archaeogeophysical studies in the USA: recent developments and prospects, *Archaeological Prospection*, **15**, 1–31.

Dalan, R. A., and Banerjee, S. K., 1998, Solving archaeological problems using techniques of soil magnetism, *Geoarchaeology: An International Journal*, **13**(1), 3–6.

De Boer, C. B., 1999, Rock-magnetic studies on the hematite, maghemite and combustion-metamorphic rocks: the quest to understand the 'hidden attraction' of rocks, Geologica Ultraiectina no. 177—Mededelingen van de Faculteit Aardwetenschappen, Universitat Utrecht, Utrecht.

Dearing, J. A., Livingstone, I. P., and Bateman, M. D., 2001, Paleoclimate records from OIS 8.0–5.4 recorded in loess paleosol sequences on the Matmata Plateau, southern Tunisia, based on mineral magnetism and new luminescence dating, *Quaternary International*, **76–7**, 43–56.

Dockrill, S. J., and Simpson, I. A., 1994, The identification of prehistoric anthropogenic soils in the northern isles using an integrated sampling methodology, *Archaeological Prospection*, **1**, 75–92.

Dunlop, D. J., 2002, Theory and application of the Day plot (M_{rs}/M_s versus H_{cr}/H_c) 2: application to data for rocks, sediments, and soils, *Journal of Geophysical Research*, **107**(B3), 1–22.

Eighmy, J. L., and Sternberg, R. S., 1990, *Archaeomagnetic dating*, The University of Arizona Press, Tucson, AZ.

Ellwood, B. B., Harrold, F., Benoist, S., Thacker, P., Otte, M., Bonjean, D., Long, G., Shahin, A., Hermann, R., and Grandjean, F., 2004, Magnetic susceptibility applied as an age–depth–climate relative dating technique using sediments from Scladina Cave, a Late Pleistocene cave site in Belgium, *Journal of Archaeological Science*, **31**, 283–93.

Evans, B. J., 1977, Magnetism and archaeology: magnetic oxides in the first American civilization, *Physica*, **86–8B**, 1091–9.

Evans, M. E., and Heller, F., 2003, *Environmental magnetism: principles and applications of enviromagnetics*, Academic Press, Amsterdam.

Fiore, D., 2014, Pinturas corporales fueguinas: una arqueología visual, in *Cazadores de mar y de tierra, estudios recientes en arqueología fueguina* (eds. J. Oría and A. Tívoli), 409–33, Museo del fin del mundo, Ushuaia, Argentina.

Fiore, D., Maier, M., Parera, S., Orquera, L., and Piana, E., 2008, Chemical analyses of the earliest pigment residues from the uttermost part of the planet (Beagle Channel region), Tierra del Fuego, southern South America, *Journal of Archaeological Science*, **35**, 3047–56.

Fischer, W. R., 1988, Microbiological reactions of iron in soils, in *Iron in soils and clay minerals* (eds. J. Stucki, B. Goodman, and U. Schwertmann), 715–48, NATO ASI Series C 217 D, Dordrecht, Reidel.

Fitzpatrick, R. W., 1985, Iron compounds as indicators of pedogenic processes: examples from the Southern Hemisphere, in *Iron in soils and clay minerals* (eds. J. Stucki, B. Goodman, and U. Schwertmann), 351–96, NATO ASI Series C 217 D, Dordrecht, Reidel.

Gajbhiye, N. S., Prasad, S., and Blaji, G., 1999, Experimental study of Hopkinson effect in single domain CoFe/sub 2/O/sub 4/ particles, *IEEE Transactions on Magnetics*, **35**(4), 2155–61.

Goguitchaichvili, A., Greco, C., and Morales, J., 2011, Geomagnetic field intensity behavior in South America between 400 AD and 1800 AD: first archeointensity results from Argentina, *Physics of the Earth and Planetary Interiors*, **186**(3), 191–7.

Goldberg, P., and Macphail, R., 2006, *Practical and theoretical geoarchaeology*, Blackwell Scientific, Oxford.

Gose, W. A., Collins, M. B., Takac, P. R., and Guy, J., 1994, Paleomagnetic studies of prehistoric burned-rock features, *Transactions of the American Geophysical Union*, **75**, 128.

Han, J., Lu, H., and Wu, N., 1996, Magnetic susceptibility of modern soils in China and its use for paleoclimate reconstruction, *Studia et Geophysica et Geodaetica*, **40**, 262–75.

Heller, F., Shen, C. D., Beer, J., Liu, X. M., Liu, T. S., Bronger, A., Suter, M., and Bonanig, G., 1993, Quantitative estimates of pedogenic ferromagnetic mineral formation in Chinese loess and paleoclimatic implications, *Earth and Planetary Science Letters*, **114**, 385–90.

Hrouda, F., 2009, Determination of field-independent and field-dependent components of anisotropy of susceptibility through standard AMS measurement in variable low fields I: theory, *Tectonophysics*, **466**(1–2), 114–22.

Hrouda, F., 2011, Models of frequency-dependent susceptibility of rocks and soils revisited and broadened, *Geophysical Journal International*, **187**(3), 1259–69.

Jackson, M., 1990, Diagenetic sources of stable remanence in remagnetized Paleozoic cratonic carbonates: a rock magnetic study, *Journal of Geophysical Research: Solid Earth*, **95**(B3), 2753–61.

Kukla, G., Heller, F., Ming, L., Chun, X., Sheng, L., and Sheng, A., 1988, Pleistocene climates in China dated by magnetic susceptibility, *Geology*, **16**(9), 811–14.

Lageras, P., and Sandgren, P., 1994, The use of mineral magnetic analyses in identifying Middle and Late Holocene agriculture, a study of peat profiles in Smaland, southern Sweden, *Journal of Archaeological Science*, **21**, 687–97.

Le Borgne, E., 1960, Influence du feu sur les propriétés magnétiques du sol et sur celles du schiste et du granite, *Annel de Géophysique*, **16**, 159–95.

Liu, Q., Deng, C., Yu, Y., Torrent, J., Jackson, M., Banerjee, S., and Zhu, R., 2005, Temperature dependence of magnetic susceptibility in an argon environment: implications for pedogenesis of Chinese loess/palaeosols, *Geophysical Journal International*, **161**(1), 102–12.

Liu, X., Rolph, T., Bloemendal, J., Shaw, J., and Liu, T., 1995, Quantitative estimates of palaeoprecipitation at Xifeng, in the Loess Plateau of China, *Palaeogeography, Palaeoclimatology*, *Palaeoecology*, **113**(2), 243–8.

Lovley, D. R., Stolz, J. F., Nord, G. L., and Phillips, E. J., 1987, Anaerobic production of magnetite by a dissimilatory iron-reducing microorganism, *Nature*, **330**(6145), 252–4.

Macphail, R. I., and Crowther, J., 2007, Soil micromorphology, chemistry and magnetic susceptibility studies at Huizui (Yiluo region, Henan Province, northern China), with special focus on a typical Yangshao floor sequence, *Bulletin of the Indo-Pacific Prehistory Association*, **27**, 93–113.

Maher, B. A., 1986, Characterisation of soils by mineral magnetic measurements, *Physics of the Earth and Planetary Interiors*, **42**, 76–92.

Maher, B. A., 1988, Magnetic properties of some synthetic sub-micron magnetites, *Geophysical Journal*, **94**, 83–96.

Maher, B. A., 1998, Magnetic properties of modern soils and Quaternary loessic paleosols: paleoclimatic implications, *Palaeogeography, Palaeoclimatology, Palaeoecology*, **137**, 25–54.

Maher, B. A., and Taylor, R. M., 1988, Formation of ultrafine-grained magnetite in soils, *Nature*, **336**, 368–71.

Maher, B. A., and Thompson, R., 1999, *Quaternary climate, environments and magnetism*, Cambridge University Press, Cambridge.

Maher, B. A., Alekseev, A., and Alekseeva, T., 2003, Magnetic mineralogy of soils across the Russian Steppe: climatic dependence of pedogenic magnetite formation, *Palaeogeography, Palaeoclimatology, Palaeoecology*, **201**, 321–41.

Maher, B. A., Thompson, R., and Zhou, L. P., 1994, Spatial and temporal reconstructions of changes in the Asian paleomonsoon: a new mineral magnetic approach, *Earth and Planetary Science Letters*, **125**, 461–71.

Marmet, E., Bina, M., Fedoroff, N., and Tabbagh, A., 1999, Relationships between human activity and the magnetic properties of soils: a case study in the medieval site of Roissy-en-France, *Archaeological Prospection*, **6**, 161–70.

Mooney, S. D., Geiss, C., and Smith, M. A., 2003, The use of mineral magnetic parameters to characterize archaeological ochres, *Journal of Archaeological Science*, **30**(5), 511–23.

Morello, F., San Román, M., and Prieto, A., 2004, Informe de actividades de sondeo en el sitio Marazzi 2 sector 1 (río Torcido, Tierra del Fuego), *Magallania*, **32**, 233–8.

Morello, F., San Román, M., Seguel, R., and Martin, F., 1998, Excavación en el sitio Marazzi 2: Sector 2—terraza superior (Río Torcido, Bahía Inútil), *Anales del Instituto de la Patagonia, Serie Ciencias Humanas*, **26**, 119–26.

Moskowitz, B. M., Jackson, M., and Kissel, C., 1998, Low-temperature magnetic behavior of titanomagnetites, *Earth and Planetary Science Letters*, **157**, 141–9.

Moskowitz, B. M., Lindsay, J., Hemphill, P., and Judson, S., 1987, A magnetic study of Etruscan Bucchero pottery: an application of rock magnetism to archaeometry, *Geoarchaeology: An International Journal*, **2**, 285–300.

Mullins, C. E., 1974, The magnetic properties of the soil and their application to archaeological prospecting, *Archaeo-Physika*, **5**, 143–347.

Muxworthy, A. R., and Williams, W., 2006, Critical single-domain/multidomain grain sizes in noninteracting and interacting elongated magnetite particles: Implications for magnetosomes, *Journal of Geophysical Research: Solid Earth*, **111**(12), 3–9.

Nami, H. G., 1995, Holocene geomagnetic excursion at Mylodon Cave, *Ultima Esperanza, Chile, Journal of Geomagnetism and Geoelectricity*, **47**, 1325–32.

Oldfield, F., Krawiecki, A., Maher, B., Taylor, J. T., and Twigger, S., 1985, The role of mineral magnetic measurements in archaeology, in *Palaeoenvironmental investigations: research design, methods and data analysis* (eds. N. Fieller, D. Gilbertson, and N. Ralph), 29–43, Symposium number 5 of the Association for Environmental Archaeology, International Series 258, British Archaeological Reports, Oxford.

Ollendorf, A. L., 1993, Changing landscapes in the American Bottom (USA): an interdisciplinary investigation with an emphasis on the late-prehistoric and early-historic periods, Ph.D. thesis, University of Minnesota.

Orgeira, M. J., and Compagnucci, R., 2006, Correlation between paleosol–soil magnetic signal and climate, *Earth, Planets and Space*, **58**(10), 1373–80.

Orgeira, M. J., and Compagnucci, R., 2010, Uso de la señal magnética de suelos y paleosuelos como función climática, *Revista de la Asociación Geológica Argentina*, **65**(4), 612–23.

Orgeira, M. J., Egli, R., and Compagnucci, R., 2011, A quantitative model of magnetic enhancement in loessic soils, *Earth's Magnetic Interior*, **1**, 361–97.

Orgeira, M. J., Favier Dubois, C., Walther, A., and Vásquez, C., 2000, Magnetismo ambiental en sedimentos holocenos tardíos de bahía San Sebastián (Tierra del Fuego): impacto climático y/o ¿señal antrópica? *Revista Cuaternario y Ciencias Ambientales*, **4**, 71–9.

Ozán, I. L., and Orgeira, M. J., 2015, Propiedades magnéticas y micromorfología de suelos en el sitio arqueológico Marazzi 2, Isla Grande de Tierra del Fuego, Chile, *Revista de la Asociación Geológica Argentina*, **72**(2), 251–64.

Ozán, I. L., French, C., Morello, F., Vásquez, C., and Luppo, T., 2015, Coastal occupations in Tierra del Fuego, southernmost South America: a geoarchaeological study of a Late Holocene hunter–gatherer context at Marazzi 2, *Geoarchaeology: An International Journal*, **30**, 465–82.

Peters, C., and Dekkers, M., 2003, Selected room temperature magnetic parameters as a function of mineralogy, concentration and grain size, *Physics and Chemistry of the Earth*, **28**, 659–67.

Roberts, A., Cui, Y., and Verosub, K., 1995, Wasp-waisted hysteresis loops: mineral magnetic characteristics and discrimination of components in mixed magnetic systems, *Journal of Geophysical Research: Solid Earth*, **100**(B9), 17 909–17 924.

Rosendahl, D., Lowe, K. M., Wallis, L. A., and Ulm, S., 2014, Integrating geoarchaeology and magnetic susceptibility at three shell mounds: a pilot study from Mornington Island, Gulf of Carpentaria, Australia, *Journal of Archaeological Science*, **49**, 21–32.

Schmidbauer, E., Mosheim, E., and Semioschkina, N., 1986, Magnetization and ^{57}Fe Mossbauer study of obsidians, *Physics and Chemistry of Minerals*, **13**, 256–61.

Tamaura, Y., Ito, K., and Katsura, T., 1983, Transformation of γ-FeO(OH) to Fe_3O_4 by adsorption of iron(II) ion on γ-FeO(OH), *Journal of the Chemical Society, Dalton Transactions*, **2**, 189–94.

Tarling, D. H., 1983, The possible utilisation of the magnetization of archaeological metallic artifacts, *Journal of Archaeological Science*, **10**, 41–2.

Taylor, R. M., Maher, B. A., and Self, P. G., 1987, Magnetite in soils: I, *The synthesis of single-domain and superparamagnetic magnetite, Clay Minerals*, **22**, 411–22.

Thompson, R., and Oldfield, F., 1986, *Environmental magnetism*, George Allen & Unwin, London.

Tite, M. S., and Mullins, C., 1971, Enhancement of the magnetic susceptibility of soils on archaeological sites, *Archaeometry*, **13**, 209–19.

Tronc, E., Belleville, P., Jolivet, J. P., and Livage, J., 1992, Transformation of ferric hydroxide into spinel by iron (II) adsorption, *Langmuir*, **8**(1), 313–19.

Tsatskin, A., and Gendler, T. S., 2016, Identification of 'red ochre' in soil at Kfar HaHoresh Neolithic site, Israel: magnetic measurements coupled with materials characterization, *Journal of Archaeological Science: Reports*, **6**, 284–92.

Tsatskin, A., and Nadel, D., 2003, Formation processes at the Ohalo II submerged prehistoric campsite, Israel, inferred from soil micromorphology and magnetic susceptibility studies, *Geoarchaeology: An International Journal*, **18**(4), 409–32.

SUPPORTING INFORMATION

Additional Supporting Information may be found in the online version of this paper at the publisher's web-site:

Figure S1. Relation between Mrs/Ms and Hcr/Hc parameters for each sample (black dots correspond to P1 profile and white dots to P2 profile). SD = single domain; PSD = pseudo-single domain; SP = superparamagnetic; MD = multi-domain (modified from Ozán and Orgeira 2015).